

Determination of the Weak Axial Vector Coupling $\lambda = g_A/g_V$ from a Measurement of the β -Asymmetry Parameter A in Neutron Beta Decay

D. Mund,^{*} B. Märkisch,[†] M. Deissenroth, J. Krempel,[‡] M. Schumann,[§] and H. Abele[¶]
Physikalisches Institut, Universität Heidelberg, Philosophenweg 12, 69120 Heidelberg, Germany

A. Petoukhov and T. Soldner^{**}
Institut Laue-Langevin, BP 156, 6, rue Jules Horowitz, 38042 Grenoble Cedex 9, France
 (Dated: November 27, 2024)

We report on a new measurement of the neutron β -asymmetry parameter A with the instrument PERKEO II. Main advancements are the high neutron polarization of $P = 99.7(1)\%$ from a novel arrangement of super mirror polarizers and reduced background from improvements in beam line and shielding. Leading corrections were thus reduced by a factor of 4, pushing them below the level of statistical error and resulting in a significant reduction of systematic uncertainty compared to our previous experiments. From the result $A_0 = -0.11996(58)$, we derive the ratio of the axial-vector to the vector coupling constant $\lambda = g_A/g_V = -1.2767(16)$.

PACS numbers: 12.15.Ji, 13.30.Ce, 14.20.Dh, 23.40.Bw

The Standard Model of weak $V - A$ interactions describes the β^- decay of the free neutron $n \rightarrow p + e + \bar{\nu}_e$ implementing the following parameters: The vector coupling constant g_V is defined by the product $G_F V_{ud}$ of the Fermi constant $G_F = g_w^2/M_W^2$, where g_w is the electroweak coupling constant and M_W is the W -boson mass, and the matrix element V_{ud} of the quark mixing Cabibbo-Kobayashi-Maskawa (CKM) matrix. The axial current is renormalized by the strong interaction at low energy. $\lambda = g_A/g_V$ is defined as the ratio of the axial vector and vector coupling constants. λ is real, if the weak interaction is invariant under time reversal. Searches for time reversal violation can be found in [1, 2].

λ , V_{ud} , and neutron's lifetime τ are interconnected by the following equation,

$$\tau^{-1} = C |V_{ud}|^2 (1 + 3\lambda^2) f^R (1 + \Delta_R), \quad (1)$$

where $C = G_F^2 m_e^5 / (2\pi^3) = 1.1613 \times 10^{-4} \text{s}^{-1}$ in $\hbar = c = 1$ units. f^R is the phase space factor [3, 4] (including the model independent radiative correction) adjusted for the current value of the neutron-proton transition energy. Δ_R [5] is the model dependent radiative correction to the neutron decay rate. Thus λ serves as input for a determination of either the CKM matrix-element V_{ud} or the lifetime τ . The Standard Model requests that the CKM matrix is unitary, a condition which is experimentally tested at the 10^{-4} level for the first row [6], and unitary tests are sensitive tools for searches for physics beyond the Standard Model. Previous determinations of V_{ud} and V_{us} raised questions about the unitarity of the CKM-matrix as discussed in [7–9]. Refs. [10–12] list several other motivations for a determination of λ and searches for new symmetry concepts in neutron beta decay. In principle, the ratio λ can be determined from QCD lattice gauge theory calculations, but the results of the best calculations vary by up to 30% [10]. The most precise experimental determination is from the β -

asymmetry in neutron decay but previous experimental results are not consistent within their uncertainties [13].

In neutron decay, the probability that an electron is emitted with angle ϑ with respect to the neutron spin polarization $P = \langle \sigma_z \rangle$ is [14]

$$W(\vartheta) = 1 + \frac{v}{c} P A \cos(\vartheta), \quad (2)$$

where v is the electron velocity. A is the parity violating β -asymmetry parameter which depends on λ . Accounting for order 1% corrections for weak magnetism $A_{\mu m}$, $g_V - g_A$ interference, and nucleon recoil, A in Eq. (2) reads [3]

$$A = A_0 (1 + A_{\mu m} (A_1 W_0 + A_2 W + A_3/W)), \quad (3)$$

with total electron energy $W = E_e/m_e c^2 + 1$ (endpoint W_0). The coefficients $A_{\mu m}$, A_1 , A_2 , A_3 are from [3] taking a different λ convention into consideration. A_0 is a function of λ ,

$$A_0 = -2 \frac{\lambda(\lambda + 1)}{1 + 3\lambda^2}, \quad (4)$$

where we have assumed that λ is real. In addition, a further small radiative correction [15] of order 0.1% must be applied.

In this letter, we present a new value for λ derived from a measurement of the β -asymmetry A with the instrument PERKEO II with strongly reduced systematic corrections and uncertainty. It was installed at the PF1B cold neutron beam position of the Institut Laue-Langevin (ILL) using a highly polarized cold neutron beam. Other correlation coefficients – the antineutrino-asymmetry parameter B [16] and the proton-asymmetry parameter C [17] – have been measured at this beam with the same instrument. Neutrons moderated by a cold source were guided via a neutron guide [18, 19] to the experiment and were then polarized using two super mirror

(SM) coated bender polarizers in crossed (X-SM) geometry [20]. An adiabatic fast passage (AFP) flipper allowed to invert the neutron spin direction. After a series of baffles for beam shaping, the transversally polarized neutron beam traversed the PERKEO II spectrometer and was absorbed in a beam dump. Two beam-line shutters, directly in front and behind the baffles, served to gain information on background [8, 21]. The main component of the PERKEO II spectrometer is a split-pair superconducting 1 T magnet providing $2 \times 2\pi$ electron guidance from the full fiducial volume to either one of two plastic scintillator detectors with size $440 \text{ mm} \times 160 \text{ mm}$ (see the lower sketch in Fig. 1 of [22]). Details on the spectrometer and electron backscatter suppression can be found in [8, 21].

From the measured electron spectra $N_i^\uparrow(E_e)$ and $N_i^\downarrow(E_e)$ in the two detectors ($i = 1, 2$) for neutron spin up and down, respectively, we define the experimental asymmetry as a function of electron kinetic energy E_e as

$$A_{\text{exp},i}(E_e) = \frac{N_i^\uparrow(E_e) - N_i^\downarrow(E_e)}{N_i^\uparrow(E_e) + N_i^\downarrow(E_e)}. \quad (5)$$

This experimental asymmetry is directly related to the asymmetry parameter A , as follows from Eq. (2) and $\langle \cos(\vartheta) \rangle = 1/2$:

$$A_{\text{exp}}(E_e) = \frac{1}{2} \frac{v}{c} A P f, \quad (6)$$

with neutron polarization P and spin flip efficiency f .

The main experimental errors of this measurement are due to *statistics*, *detector response*, *neutron spin polarization*, and *background subtraction*, see Tab. I. The four-fold intensity of the PF1B beam compared to the previous PF1 beam is used to enhance both statistics and systematics. The detected neutron decay rate within the fiducial volume was 375 s^{-1} .

Polarization: The X-SM geometry efficiently suppresses garland reflections, resulting in a nearly wavelength- and angle-independent beam polarization. This dramatically reduces systematic uncertainties for determining the average beam polarization. Polarization measurements were performed employing time-of-flight behind a chopper to gain wavelength resolution. A second AFP flipper and two Schärpf polarizers [23, 24] in X-SM geometry as analyzers were used to measure the spin flip efficiency and for a rough determination of the beam polarization. Measurements in front and behind the PERKEO II spectrometer yielded consistent results. The absolute polarization was determined using a series of opaque ^3He spin filter cells of different pressures and lengths, covering the wavelength range from 2 \AA to 20 \AA , see Fig. 1. Cells with both orientations of the ^3He spin were used to increase sensitivity [25]. Wavelength averages were calculated taking into account the decay probability which is proportional to the measured capture spectrum. The spatial dependence was verified by measurements at five different positions across the neutron beam

and found to be negligible. The resulting averages were $P = 99.7(1)\%$ and $f = 100.0(1)\%$. Note that opaque ^3He spin filters have an intrinsic accuracy of better than 10^{-4} for polarization analysis [26].

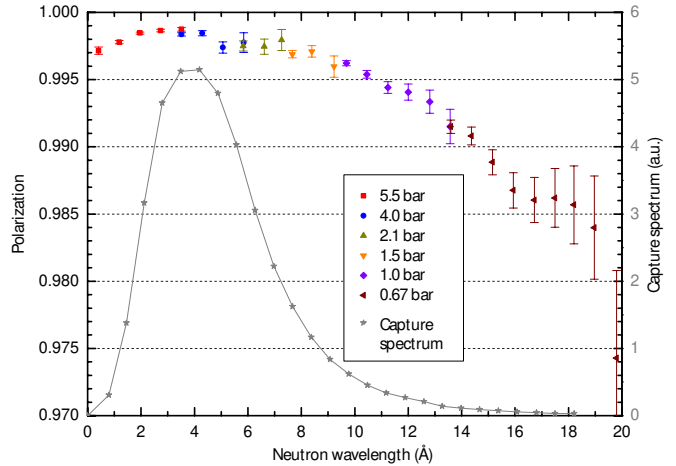


FIG. 1. Neutron polarization in the center of the PERKEO II beam. In order to cover the full spectrum with opaque ^3He cells, 6 cells were used, with lengths of 25 cm or 10 cm and different pressures. In the legend, the effective pressures for a 10 cm cell are given. (Color online)

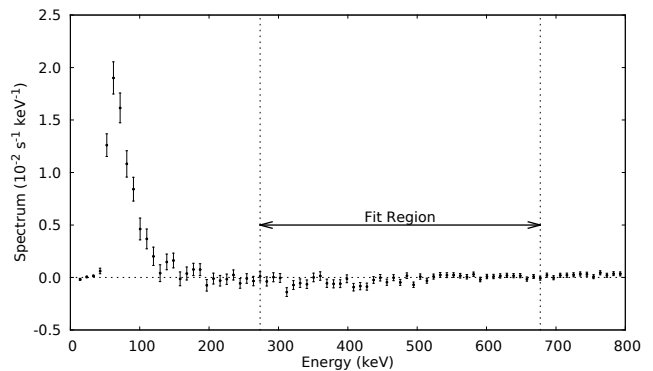


FIG. 2. Difference of spectra in detector 1 for the second and the first beam line shutter closed, a measure for the background produced by the collimation system. The main part of the background is low energetic. In detector 2, the background looks similar.

Background: The magnetic field of PERKEO II collects all electrons from the decay volume ($100 \times 80 \times 270 \text{ mm}^3$) and thus assures a high signal-to-background ratio, together with thin plastic scintillators (5 mm thickness). Environmental background was reduced by lead and iron shielding and measured with the first beam-line shutter closed. It was not constant in time due to shutter operations of neighboring instruments. Changes were monitored by NaI scintillators placed outside the PERKEO II shielding, and shutter operations were registered. For the analysis, only data sets with constant environmen-

tal background were used. This procedure reduces the data set to 5.9×10^7 neutron decay events and increases the relative statistical error to 3.8×10^{-3} (compared to 2.6×10^{-3} in the preliminary analysis of [10, 27]). The trigger rate of 500 s^{-1} comprises about 120 s^{-1} from environmental background. The signal-to-background ratio in the fit region was better than 8 : 1.

Beam-related background is more difficult to address. In the PERKEO II spectrometer, the β -detectors are far off the beam at a transverse distance of 960 mm. The beam line was optimized to place the last beam-defining baffle further away from the spectrometer than it was in our previous measurement [8]. The beam stop was positioned 4 m downstream of the decay volume. Baffles and beam stop were made from enriched ^6LiF ceramics. The baffles' lead supports shielded capture gammas (about 10^{-4} per capture). Supports and beam line were protected against scattered neutrons by ^6LiF rubber or boron glass. Halo baffles (not touching the beam) absorbed scattered neutrons close to the beam. Lead shielding was placed around the spectrometer to assure that gamma rays are scattered at least twice before they can reach a detector. In ^6LiF , about 10^{-4} fast neutrons are produced per capture from (t, n) reactions [28]. These neutrons were shielded by borated polyethylene (or, inside the beam stop vacuum, Plexiglas surrounded by borated glass) and secondary gammas by lead. The beam-related background was estimated from measurements with the two shutters using an extrapolation procedure described in [22] and confirmed by additional tests with external background sources. Compared to the previous measurement [8] of $1/200$, it was reduced to $1/1700$ of the electron rate in the fit region, which corresponds to $0.11(2) \text{ s}^{-1}$, see Fig. 2, resulting in a correction of $1(1) \times 10^{-3}$. The assumed relative uncertainty of 100% is a very conservative estimate for this background extrapolation method.

Detector response: The plastic scintillators were read out by four photomultipliers per detector. Signals were integrated by charge-to-digital converters over a time interval that includes signals from backscattering. Trigger time differences between the detectors were registered to attribute the event in case of backscattering. The detector response function was determined and the detector stability was checked regularly using four mono-energetic conversion electron sources (^{109}Cd , ^{113}Sn , ^{207}Bi , and ^{137}Cs) on $10 \mu\text{g}/\text{cm}^2$ carbon backings, which were remotely inserted into the spectrometer. The branching ratios for K, L, M and N conversion electrons and the corresponding Auger electrons have been measured separately with silicon detectors [29] and were taken into account in the corresponding fit functions. Drift in the detector gain was smaller than 1% and corrected for. The detectors showed a small non-linearity at low energy. The largest systematic uncertainty is caused by the spatial non-uniformity of the detector response. Collected light

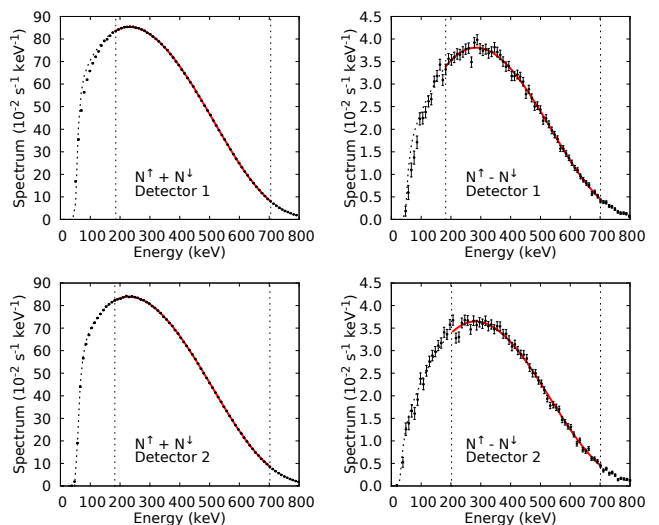


FIG. 3. Neutron β^- -spectra after adding or subtracting opposite neutron spin orientations N^\uparrow and N^\downarrow for detector 1 and detector 2, respectively. The solid curve shows a fit to the spectra in the range indicated by the vertical lines. The spectra ($N^\uparrow - N^\downarrow$) are per se free of background.

Type	Correction (10^{-3})	Uncertainty (10^{-3})
Neutron polarization	3.0	1.0
Spin flip efficiency	0.0	1.0
Background	1.0	1.0
Detector response	0.0	2.5
Electron backscattering	0.25	0.04
Edge effect (1)	(-1.6)	0.5
Magnetic mirror effect	0.6	0.2
Dead time (2)	(-1.2)	0.1
Radiative Correction	0.9	0.5
Statistics	0.0	3.8

TABLE I. Summary of corrections and uncertainties to the beta asymmetry $\Delta A_0/A_0$. (1) is included in the fit function, (2) is measured by the data acquisition system and accounted for in the data set.

output for electrons detected in the center of the scintillator was about 5% lower than for electrons detected at the ends. This spatial dependence was mapped using different calibration sources and was found to follow the expected cosh dependence. The detector gain, which has been used for the fit to the asymmetry parameter A of Eq. (6) and Fig. 4, was obtained by a fit to the spectrum ($N^\uparrow - N^\downarrow$), see Fig. 3, which is background free. A fit to ($N^\uparrow + N^\downarrow$) would yield a different gain resulting in a significant dependence of the asymmetry A on the lower limit of the fit region for detector 2.

Backscattering: By using the second detector as veto detector and carefully analyzing events with energies be-

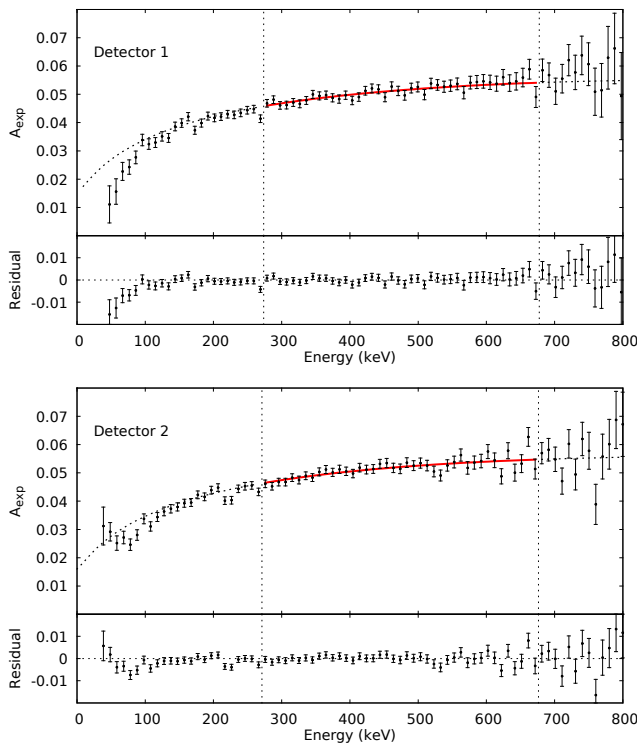


FIG. 4. Fit and residuals to the experimental asymmetry A_{exp} for detector 1 and detector 2. The solid curve shows the fit interval, whereas the dotted curve shows an extrapolation to higher and lower energies.

low the trigger threshold on one detector [30], the fraction of wrongly attributed electrons in the fit region was deduced to be $1.3(3) \times 10^{-4}$ per detector, corresponding to a correction of $0.25(4) \times 10^{-3}$ compared to $2.0(1.7) \times 10^{-3}$ in the previous experiment [8].

Edge effect: The length of the decay volume is defined by electron absorbing aluminum baffles. The absorption depends on the radius of gyration and thus on the energy of the electron. The resulting correction can be reliably calculated and is included in the fit function.

Mirror effect: Electrons can be reflected on an increasing magnetic field, leading to detection in the wrong detector. This magnetic mirror effect, due to a small displacement between neutron beam and the maximum of the magnetic field, caused a difference of 1.4% between the asymmetries measured in the two detectors. Most of this effect cancels by averaging the two detectors. The remaining correction, due to the spacial extension of the neutron beam, was calculated from the measured magnetic field geometry and neutron beam profile.

The experimental function $A_{\text{exp},i}(E_e)$ and a fit with a single free parameter λ are shown in Fig. 4 for both detectors. The fit interval was chosen such as to minimize effects due to non-linearity of the detector and unrecognized background. From the experimental asymme-

tries we get $|A_0| = 0.11846(64)_{\text{stat}}$ for detector 1 and $|A_0| = 0.12008(64)_{\text{stat}}$ for detector 2. All subsequent corrections and uncertainties entering the final determination of A_0 are listed in Tab. I. After averaging and correcting for those small and mostly experimental systematic effects, we obtain

$$A_0 = -0.11996(45)_{\text{stat}}(37)_{\text{sys}} = -0.11996(58) \quad \text{and} \\ \lambda = -1.2767(16). \quad (7)$$

This value is consistent with our earlier result [8] of $A_0 = -0.1189(7)$. The combined results of the new and our previous [8, 21] experiments are

$$A_0 = -0.11951(50) \quad \text{and} \quad \lambda = -1.2755(13). \quad (8)$$

In the average Eq. (8) we have accounted for correlations of systematic errors in the experiments. Conservatively, errors concerning detector calibration and uniformity, background determination, edge effect and the radiative correction were considered correlated on the level of the smallest error of all three experiments.

Other experiments [31–33] gave significantly lower values for $|\lambda|$. However, in all these experiments large corrections had to be applied for neutron polarization, magnetic mirror effects, solid angle, or background, which were in the 15% to 30% range. In our present experiment, all individual corrections are below 3×10^{-3} and the sum of their absolute values is below 1%. We therefore use only the value given in Eq. (8) for further discussion. The determination of $\lambda = -1.27590^{+0.00409}_{-0.00445}$ by the UCNA collaboration [34] is in agreement with this result, albeit with a larger error.

Assuming the $V - A$ structure of the Standard Model, neutron lifetime can be determined using the $\overline{\mathcal{F}t}$ value from nuclear beta decay

$$\tau_n = \frac{2}{\ln 2} \frac{\overline{\mathcal{F}t}}{f_R(1 + 3\lambda^2)}, \quad (9)$$

where the phase space factor $f_R = 1.71385(34)$ [4] includes radiative corrections. We use our result Eq. (8) and $\overline{\mathcal{F}t} = 3071.81(83)$ [6] to derive the neutron lifetime

$$\tau_n = 879.4(1.6) \text{ s}. \quad (10)$$

This result is in agreement with and nearly as precise as the current world average $\tau_n = 881.9(1.3) \text{ s}$ [12] that includes a scale factor of 2.5.

The authors would like to thank Markus Brehm for his contribution during the preparation of the measurement and Anthony Hillaret for his contribution during the beam time, and several services of the Physikalisches Institut, University of Heidelberg, and of the ILL, in particular the Neutron Optics Group. This work was supported by the Priority Programme SPP 1491 of the Austrian FWF and the German DFG, contracts FWF

I529-N20, MA 4944/1-1 and SO 1058/1-1, and the German BMBF, contract No. 06HD187.

* New family name: *Schirra*.

† maerkisch@physi.uni-heidelberg.de

‡ Now at ETH Zürich, Institut für Teilchenphysik, Schafmattstr. 20, 8093 Zürich, Switzerland

§ Now at Universität Zürich, Winterthurerstr. 190, 8057 Zürich, Switzerland

¶ Now at Atominstitut, Technische Universität Wien, Stationalallee 2, 1020 Wien, Austria; abele@ati.at

** soldner@ill.fr

- [1] T. Soldner *et al.*, Phys. Lett. B **581**, 49 (2004).
 [2] H. P. Mumm *et al.*, Phys. Rev. Lett. **107**, 102301 (2011).
 [3] D. H. Wilkinson, Nucl. Phys. A **377**, 474 (1982).
 [4] G. Konrad *et al.*, in *Proceedings of the 5th International BEYOND 2010 Conference, Cape Town, South Africa (2010)* (World Scientific, 2011) pp. 660–672, arXiv:1007.3027 [nucl-ex].
 [5] W. J. Marciano and A. Sirlin, Phys. Rev. Lett. **96**, 032002 (2006).
 [6] J. C. Hardy and I. S. Towner, Phys. Rev. C **79**, 055502 (2009).
 [7] I. Towner *et al.*, (1995), arXiv:nucl-th/9507005.
 [8] H. Abele *et al.*, Phys. Rev. Lett. **88**, 211801 (2002).
 [9] H. Abele and D. Mund, eds., *Quark mixing, CKM unitarity* (2003) arXiv:hep-ph/0312124 [hep-ph].
 [10] H. Abele, Prog. Part. Nucl. Phys. **60**, 1 (2008).
 [11] N. Severijns and O. Naviliat-Cuncic, Annu. Rev. Nucl. Part. Sci. **61**, 23 (2011).
 [12] D. Dubbers and M. G. Schmidt, Rev. Mod. Phys. **83**, 1111 (2011), arXiv:1105.3694v1 [hep-ph].
 [13] K. Nakamura and others (Particle Data Group), J. Phys. G **37**, 075021 (2010), and 2011 partial update.
 [14] J. D. Jackson, S. B. Treiman, and H. W. Wyld, Phys. Rev. **106**, 517 (1957).
 [15] F. Glück and K. Toth, Phys. Rev. D **46**, 2090 (1992).
 [16] M. Schumann *et al.*, Phys. Rev. Lett. **99**, 191803 (2007).
 [17] M. Schumann *et al.*, Phys. Rev. Lett. **100**, 151801 (2008).
 [18] H. Häse *et al.*, Nucl. Inst. & Meth. A **485**, 453 (2002).
 [19] H. Abele *et al.*, Nucl. Inst. & Meth. A **562**, 407 (2006).
 [20] M. Kreuz *et al.*, Nucl. Inst. & Meth. A **547**, 583 (2005).
 [21] H. Abele *et al.*, Phys. Lett. B **407**, 212 (1997).
 [22] J. Reich *et al.*, Nucl. Inst. & Meth. A **440**, 535 (2000).
 [23] O. Schärpf, Physica B **156**, 639 (1989).
 [24] O. Schärpf and N. Stüsser, Nucl. Inst. & Meth. A **284**, 208 (1989).
 [25] O. Zimmer, Phys. Lett. B **461**, 307 (1999).
 [26] T. Soldner *et al.*, (2011), Institut Laue Langevin, experimental report 3-07-235.
 [27] D. Mund, *Messung der Betaasymmetrie A im Neutronenzerfall*, Dissertation, Universität Heidelberg (2006).
 [28] M. Lone *et al.*, Nucl. Inst. & Meth. **174**, 521 (1980).
 [29] H. Abele *et al.*, Phys. Lett. B **316**, 26 (1993).
 [30] M. Schumann and H. Abele, Nucl. Inst. & Meth. A **585**, 88 (2008).
 [31] B. Yerozolimsky *et al.*, Phys. Lett. B **412**, 240 (1997).
 [32] P. Liaud *et al.*, Nucl. Phys. A **612**, 53 (1997).
 [33] P. Bopp *et al.*, Phys. Rev. Lett. **56**, 919 (1986).
 [34] J. Liu *et al.*, Phys. Rev. Lett. **105**, 181803 (2010).